Supporting Information

Ge et al. 10.1073/pnas.1109597108

SI Text

Selection Criteria of F-D Curves Recorded upon Unfolding of Single BetP Molecules. WT BetP is composed of 595 aa and the longest F-D curves reproducibly recorded on WT BetP exhibited lengths ranging between 130 and 160 nm (Fig. 1*B*, Fig. S1). SMFS on α-helical membrane proteins showed that the last force peak of such longest F-D curves detected interactions that have been established by the last terminal region remaining embedded in the membrane (1). If the AFM stylus pulls one terminal end of BetP and unfolds all stable structural segments until the opposing terminal region established the final unfolding barrier we reveal a stretched polypeptide of ≈360–500 aa. This length of the stretched polypeptide corresponds to a pulling distance of ≈130–180 nm. Thus, we could conclude that the 130–160 nm long F-D curves (Fig. S1) were obtained upon unfolding BetP from either one of its terminal ends. To ensure that we analyzed only BetP molecules that have been attached to the AFM stylus by their N- or C-terminal end we applied this length criterion to select the F-D curves.

BetP Attaches Nonspecifically with the N-Terminal End to the AFM Stylus. The force peaks of the F-D spectra (Fig. 1*B*, Fig. S1) reflect interactions, which have been established within the membrane protein (1). The attachment of the BetP to the AFM stylus occurred nonspecifically. Because we recorded only one characteristic F-D pattern we must assume that BetP preferentially attached with one of its terminal ends to the AFM stylus. To identify from which terminal end the nonspecific attachment of BetP occurred, we performed SMFS experiments on two shortened forms of BetP. BetPΔC45 was a mutant lacking 45 aa of the C-terminal end and BetPΔN exhibited a N-terminal end truncated by ≈35 aa after aminopeptidase (AP) treatment. Comparative SDS-PAGE analysis for the AP cleaved and intact BetP validated successful cleavage of the transporter (Fig. S2).

The position of the last force peak of F-D curves recorded for WT BetP and BetPΔN allowed estimating the maximum length of their stretched polypeptides. WT BetP reconstituted into the 1-palmitoyl-2-oleoyl-phosphatidylglycerol (POPG) lipid membranes showed a last force peak at an average pulling distance of 139 ± 3 nm (Fig. S3*A*), which fitted by the worm-like-chain (WLC) model corresponds to a 527 ± 11 aa long stretched polypeptide. In contrast to WT BetP and BetPΔC45, the average maximum length of F-D curves recorded of BetPΔN55-60 was significantly shortened to 495 ± 8 aa (Fig. S3*B*). The length difference of ≈32 aa matched the truncation of the N-terminal end by ≈35 aa estimated by SDS-PAGE (Fig. S2). Irrespective of its truncated N-terminal end, the unfolding spectra of BetPΔN showed similar force peak patterns such as observed for WT BetP and BetPΔC45 (Fig. S3). However, compared to WT BetP the positions off all major force peaks were shifted by ≈32 aa. Possible minor peaks at too close distance (<15 nm) could possibly not be detected because this pulling distance is usually masked by unspecific interactions occurring between AFM stylus and membrane (1,2). This shift of the force spectra towards shorter contour lengths leads to the conclusion that in all experiments shown in Fig. S1 and S3 the AFM stylus pulled the N-terminal end of BetP.

Applying a Membrane Compensation to Locate Interactions within the Membrane or the Membrane Surface Opposite to the Pulling AFM Stylus. In some cases the contour length suggested that the interaction anchoring the unfolded polypeptide was located at the membrane surface (periplasm) opposite to the pulling AFM stylus. To locate this interaction, the thickness of the membrane (≈4 nm) was added to the measured contour length of the unfolded polypeptide. This "membrane compensation" called procedure (1, 3) adds ≈11 aa to the contour length of the unfolded polypeptide locates the interaction inside the membrane (Fig. 2). In other cases the anchor of the polypeptide had to be assumed to locate in the membrane. Depending on the location we added *n* aa to the contour length with n*0.36 nm equals the vertical position of the anchor in the membrane.

1. Kedrov A, Janovjak H, Sapra KT, Muller DJ (2007) Deciphering molecular interactions of native membrane proteins by single-molecule force spectroscopy. *Annu Rev Biophys Biomol Struct* 36:233–260.
2. Oesterhelt F, Oesterhelt D, Pfeiffer M, Engel A, Gaub HE, Müller DJ (2000) Unfolding pathways of individual bacteriorhodopsins. *Science* 288:143–146.
3. Muller DJ, et al. (2002) Stability of bacteriorhodopsin alpha-helices and loops analyzed by single-molecule force spectroscopy. *Biophys J* 83:3578–3588.

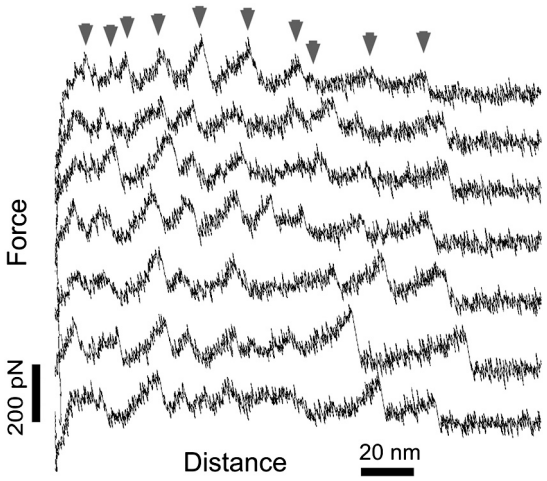

Fig. S1. Single force-distance curves recorded upon unfolding of WT BetP using SMFS. Force-distance (*F–D*) curves recorded upon unfolding of individual BetP protomers exhibiting lengths between 130 and 150 nm. Force peaks (pointed out by arrows) correspond to interactions established by unfolding intermediates of BetP. The buffer conditions were 500 mM NaCl, 50 mM Tris-HCl, pH 7.5.

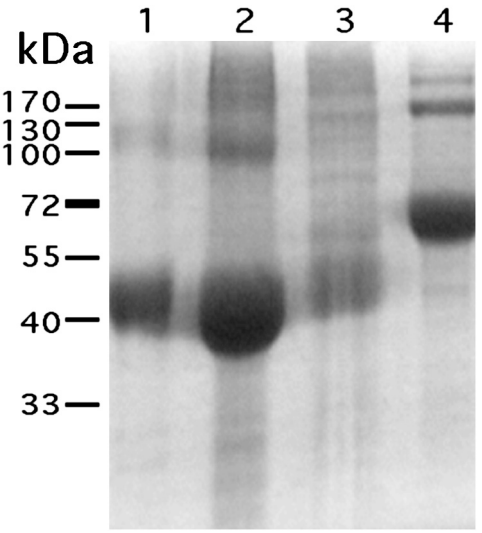

Fig. S2. 10% SDS-PAGE electrophoresis of different BetP forms. Lanes show WT BetP migrating at 67 kDa (lane 4), aminopeptidase (AP I) treated WT BetP migrating at 48 kDa (lane 3), mutant BetP lacking 45 aa at the C terminus (BetPΔC45) migrating at 46 kDa (lane 1), and mutant BetP lacking ≈35 aa at the N-terminal end (BetPΔN) migrating at 41 kDa (lane 2). pASK-IBA5 *betPΔC45*, *betP* with a fused N-terminal Strep-tag II (WSHPQFEK) was constructed as described (1) and transformed into *Escherichia coli* DH5α-T1 strain (Invitrogen). Lyophilized AP I 1 [AP I from *Streptomyces gryseus* (leucine AP IV) was purchased from Sigma] was prepared fresh in cleavage buffer consisting of 100 mM Tris/HCl, pH 7.5. Before cleavage two-dimensional crystals of reconstituted BetP were checked for diffraction by cryoelectron microscopy, spinned down at 5,000 rpm for 10 min at room temperature, resuspended in 100 mM Tris/HCl and 3 mM NaN_3, pH 7.5, and once more checked by cryoelectron microscopy. Only slight aggregation was detected. For successful N-terminal cleavage of the BetP we used an AP I to protein ratio 1:30 (w/w). Cleavage was carried out at a room temperature for 24 h and cleavage buffer was exchanged several times to remove excess AP I. Two-dimensional BetP crystals were still diffracting when checked by cryoelectron microscopy after cleavage. The efficiency of the BetP cleavage at the N terminus was validated by Western blot against a N-terminal fused StrepII tag (data not shown).

1 Schiller D, Rubenhagen R, Kramer R, Morbach S (2004) The C-terminal domain of the betaine carrier BetP of *Corynebacterium glutamicum* is directly involved in sensing K^+ as an osmotic stimulus. *Biochemistry* 43:5583–5591.

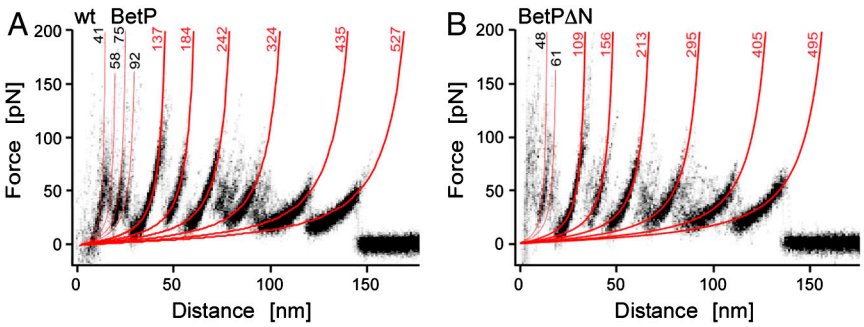

Fig. S3. F-D spectra of WT BetP and BetPΔN. Superimpositions of F-D spectra recorded of WT BetP (*A*, $n = 30$) and BetP having a truncated (≈35 aa) N terminus (BetPΔN) (*B*, $n = 30$) being reconstituted in native POPG lipids. Experiments were conducted in 200 mM NaCl, 50 mM Tris-HCl, pH 7.5. Red curves represent worm-like-chain (WLC) fits of the force peaks. Every number at the upper end of a WLC fit denotes the contour length of the unfolded and stretched polypeptide (given in amino acids).

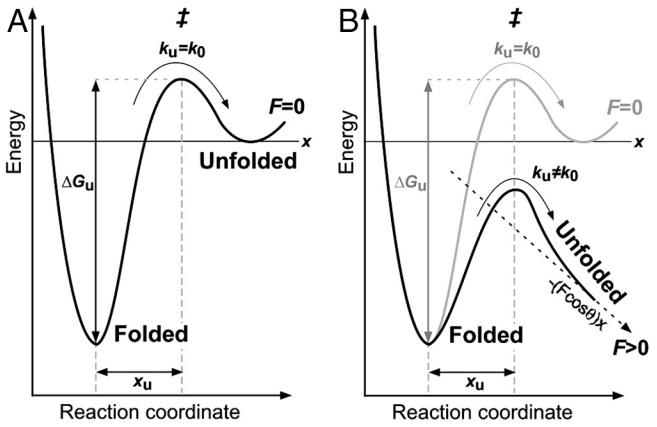

Fig. S4. Conceptual energy barrier describing the stability and unfolding of a protein exposed to an externally applied force. The energy barriers were adopted according to the Bell-Evans theory (1–3). (*A*) Two-state model describing the mechanical unfolding experiments. The energy potential exhibits one energy barrier separating the folded low-energy state from the unfolded state. ΔG_u gives the activation energy for unfolding, x_u describes the distance from the folded to the transition state, ‡, and k_u gives the transition rate for crossing the energy barrier. In absence of externally applied forces the thermal transition rate equals that of equilibrium k_0. (*B*) Application of an external force, *F*, changes the thermal likelihood of reaching the top of the energy barrier. It is assumed, that the thermally averaged projection of the energy profile along the pulling direction is tilted by the mechanical energy $(-F_{\cos}\theta)x$ (short-dashed line) without changing the distance, x_u, of the folded state relative to the energy barrier. θ gives the angle of the externally applied force relative to the molecular reaction coordinate *x*. This tilt decreases the energy barrier (black energy potential). At smaller applied forces, the thermal contribution to overcome the energy barrier is higher, and therefore, the mechanical energy required to overcome the barrier is smaller. At increasingly applied force, the lifetime of the folded state reduces.

1 Bell GI (1978) Models for the specific adhesion of cells to cells. *Science* 200:618–627.
2 Evans E, Ritchie K (1997) Dynamic strength of molecular adhesion bonds. *Biophys J* 72:1541–1555.
3 Evans E (2001) Probing the relation between force–lifetime–and chemistry in single molecular bonds. *Annu Rev Biophys Biomol Struct* 30:105–128.

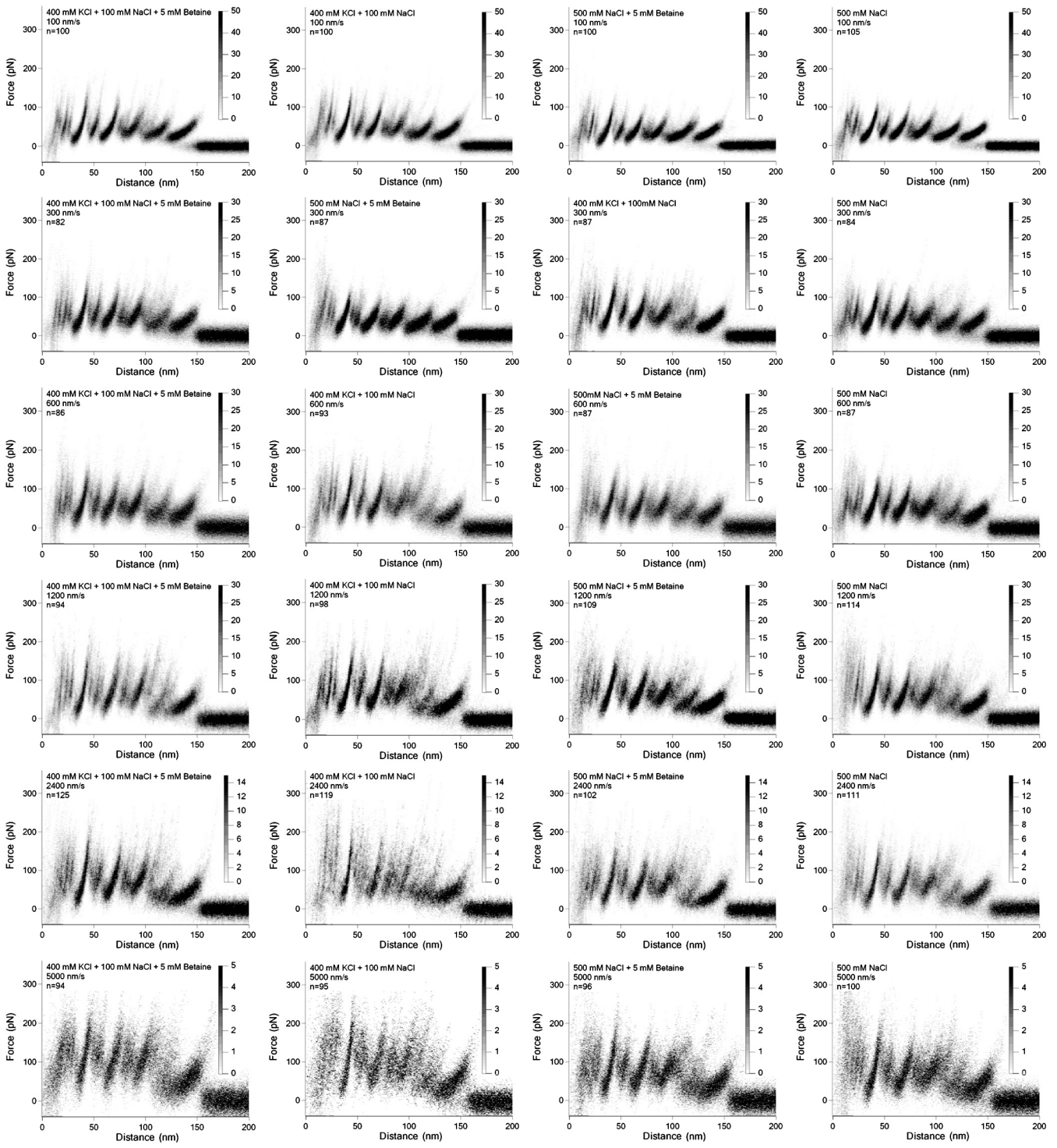

Fig. S5. Superimpositions of F-D curves recorded upon unfolding of WT BetP at six different pulling speeds and four different buffer solutions. Pulling speeds used to probe the interactions occurring during unfolding of single BetP molecules were 100, 300, 600 1,200, 2,400, and 5,000 nm/s. The buffer conditions were first column (400 mM KCl, 100 mM NaCl, 5 mM betaine, 50 mM Tris-HCl, pH 7.5), second column (400 mM KCl, 100 mM NaCl, 50 mM Tris-HCl, pH 7.5), third column (500 mM NaCl, 5 mM betaine, 50 mM Tris-HCl, pH 7.5), and last column (500 mM NaCl, 50 mM Tris-HCl, pH 7.5). BetP characterized has been reconstituted into native *E. coli* lipids. *n* indicates the number of F-D curves superimposed.

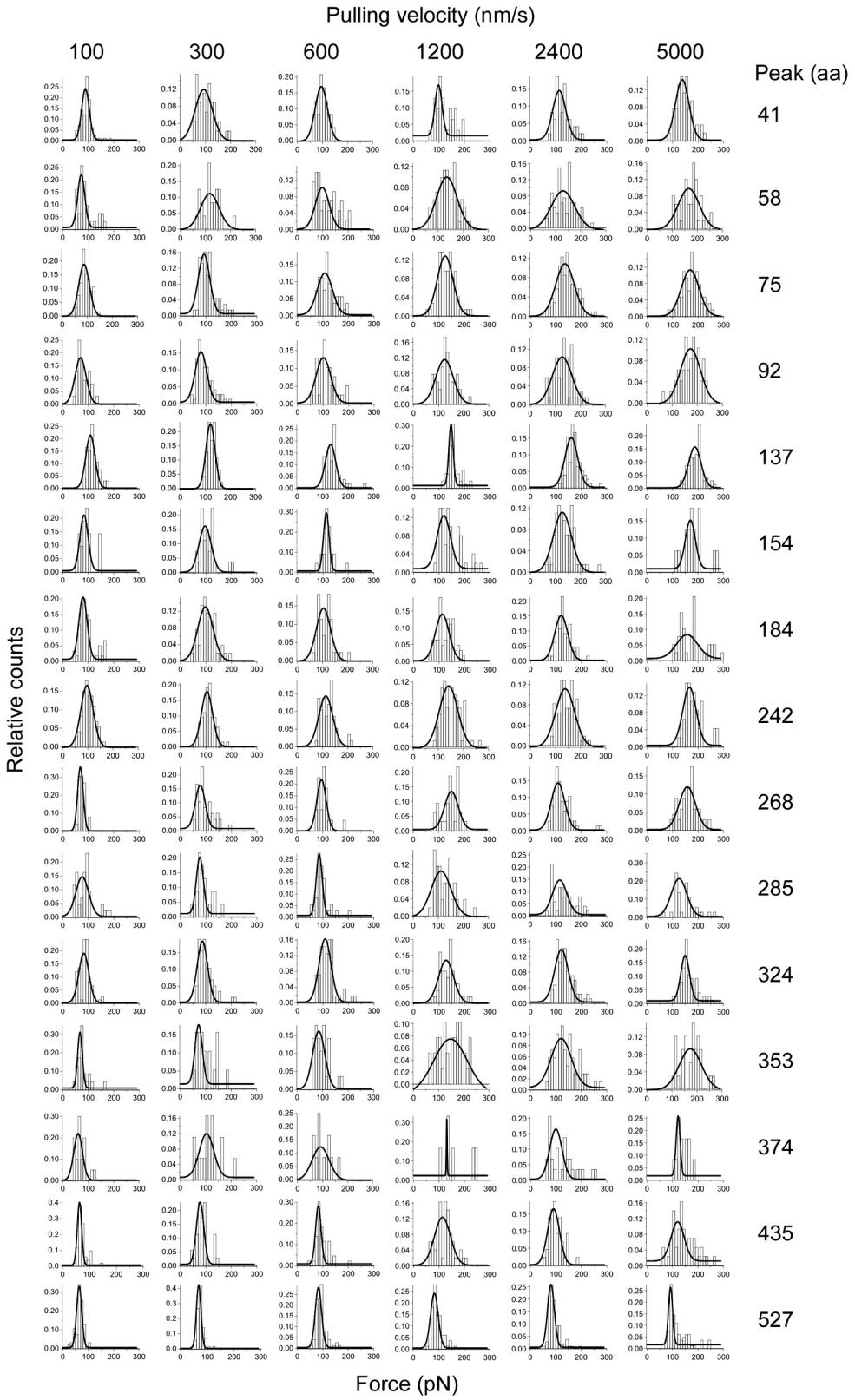

Fig. S6. Distributions of force peaks recorded upon unfolding of substrate-free BetP in the presence of 100 mM NaCl, 400 mM KCl, and 5 mM betaine. Histograms show force distributions for every force peak over six different pulling velocities (100, 300, 600 1,200, 2,400, and 5,000 nm/s). The bin size of the histograms is 10 pN. Black lines represent Gaussian fits of force distributions. The BetP characterized has been reconstituted into native *E. coli* lipids. Data was recorded in 100 mM NaCl, 400 mM KCl, 5 mM betaine, 50 mM Tris-HCl, pH 7.5.

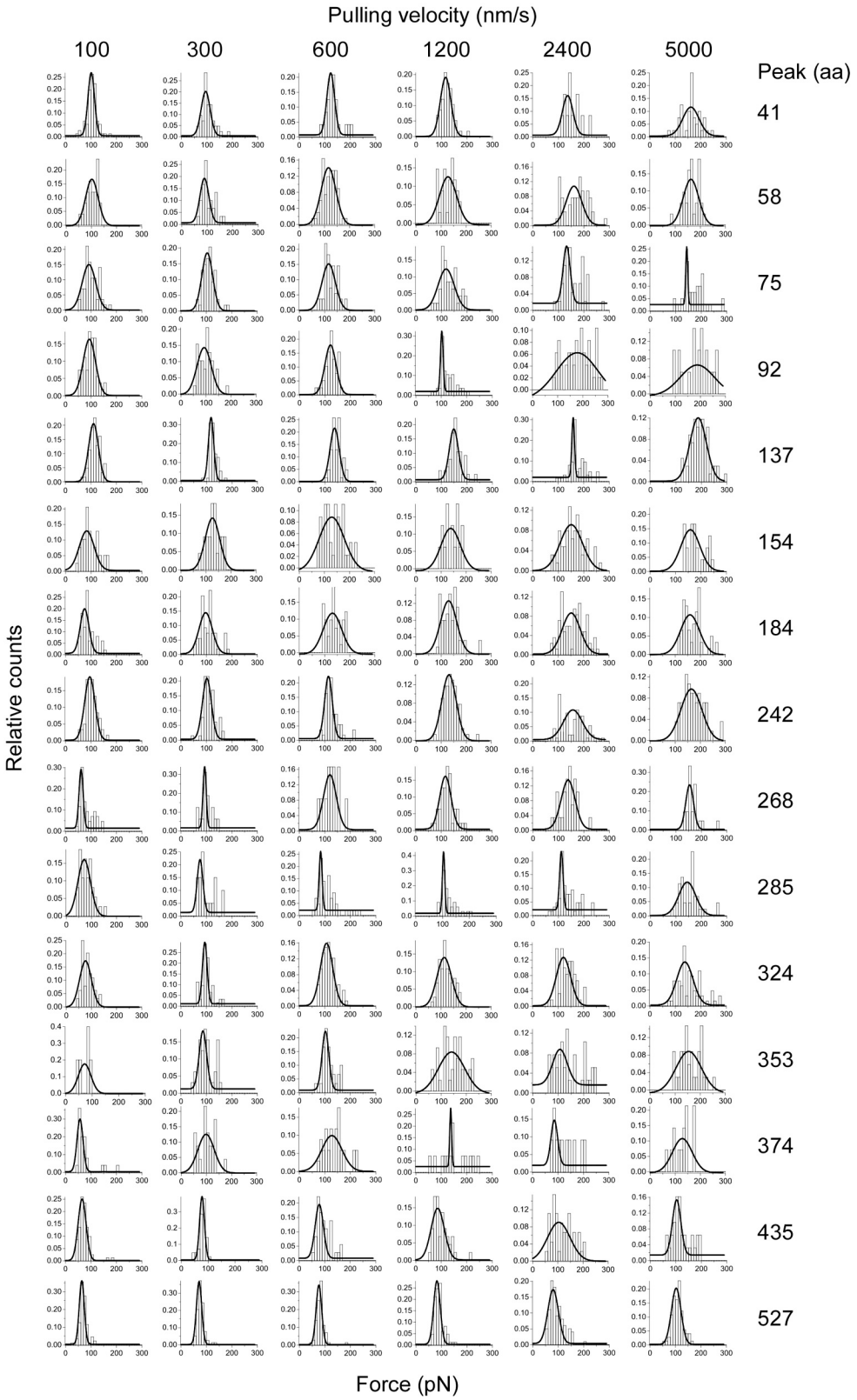

Fig. S7. Force distributions of force peaks recorded upon unfolding of substrate-free BetP in the presence of 100 mM NaCl and 400 mM KCl. Histograms show force distributions for every force peak over six different pulling velocities (100, 300, 600, 1,200, 2,400, and 5,000 nm/s). The bin size of the histograms is 10 pN. Black lines represent Gaussian fits of force distributions. The BetP characterized has been reconstituted into native *E. coli* lipids. Data was recorded in 100 mM NaCl, 400 mM KCl, 50 mM Tris-HCl, pH 7.5.

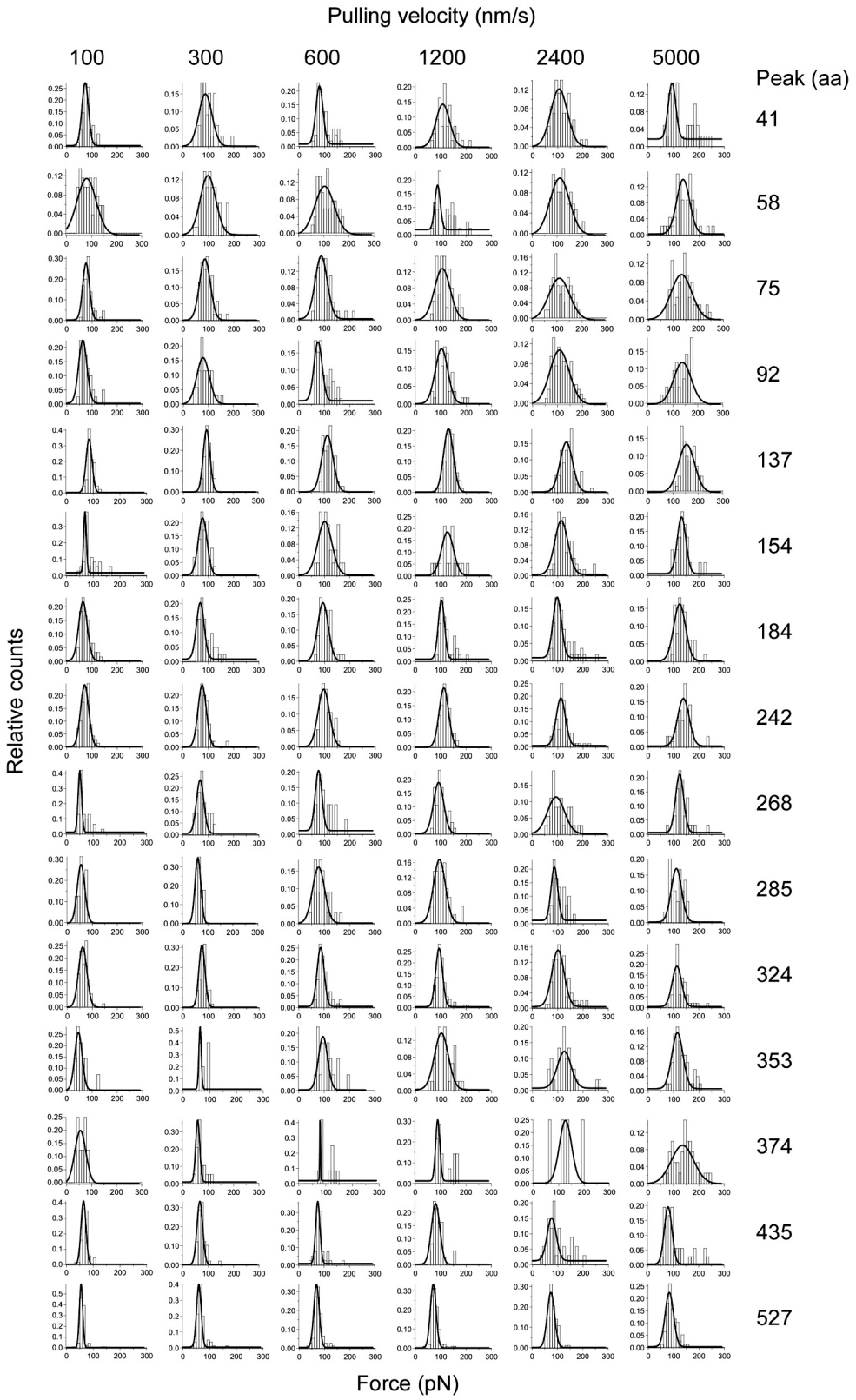

Fig. S8. Force distributions of force peaks recorded upon unfolding of substrate-free BetP in the presence of 500 mM NaCl and 5 mM betaine. Histograms show force distributions for every force peak over six different pulling velocities (100, 300, 600, 1,200, 2,400, and 5,000 nm/s). The bin size of the histograms is 10 pN. Black lines represent Gaussian fits of force distributions. The BetP characterized has been reconstituted into native *E. coli* lipids. Data was recorded in 500 mM NaCl, 5 mM betaine, 50 mM Tris-HCl, pH 7.5.

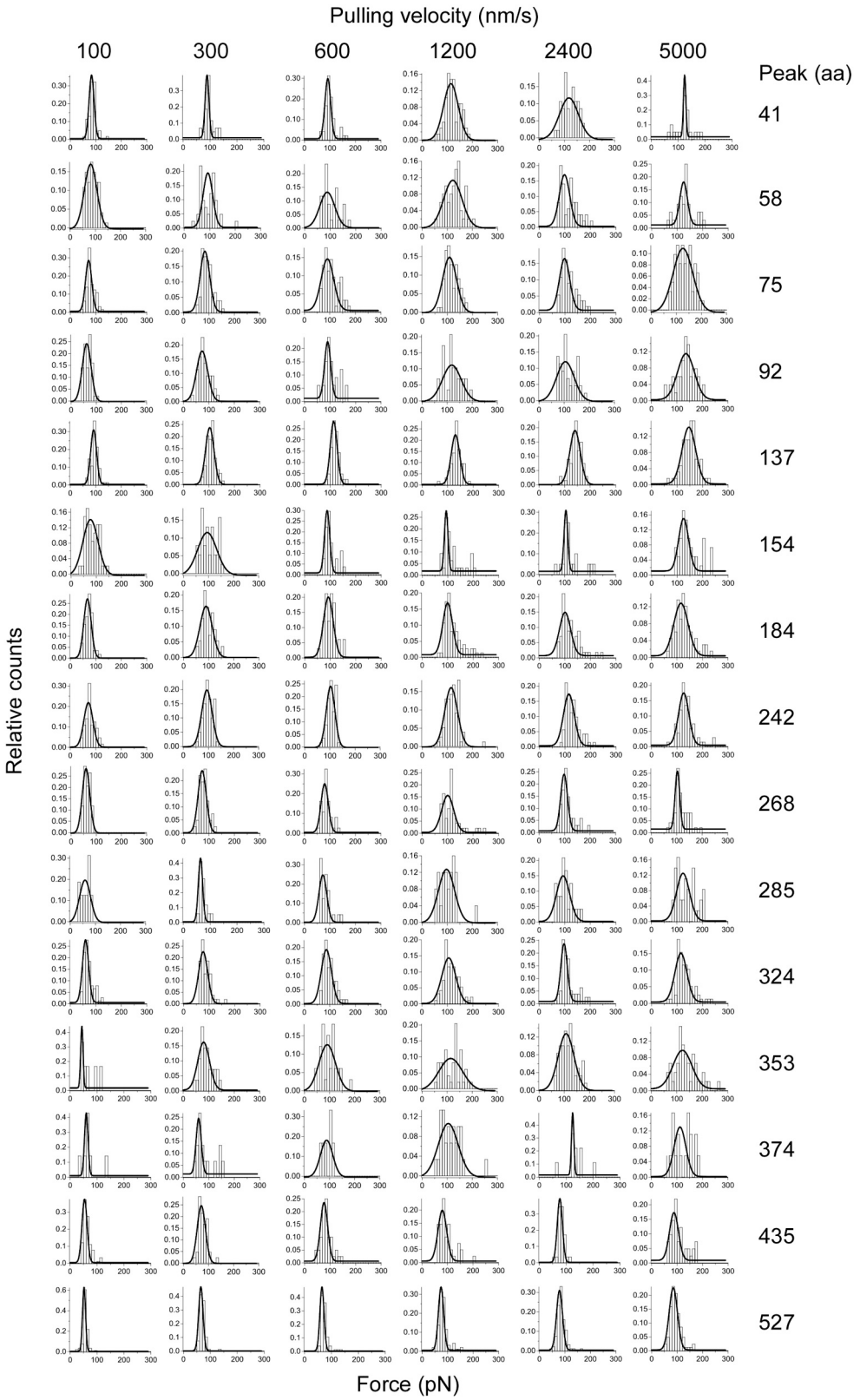

Fig. S9. Force distributions of force peaks recorded upon unfolding of substrate-free BetP in the presence of 500 mM NaCl. Histograms show force distributions for every force peak over six different pulling velocities (100, 300, 600, 1,200, 2,400, and 5,000 nm/s). The bin size of the histograms is 10 pN. Black lines represent Gaussian fits of force distributions. The BetP characterized has been reconstituted into native *E. coli* lipids. Data was recorded in 500 mM NaCl, 50 mM Tris-HCl, pH 7.5.

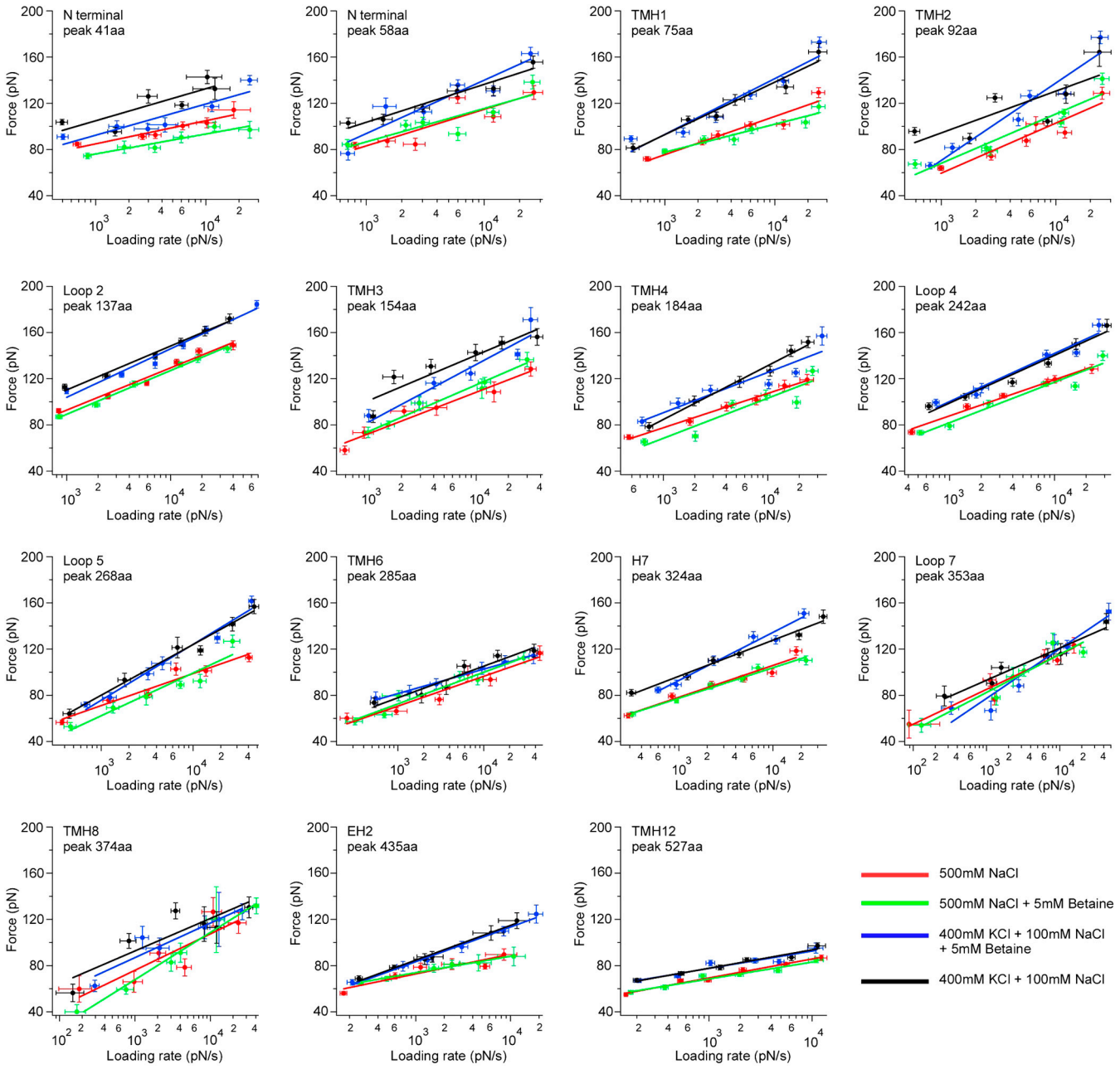

Fig. S10. Dynamic SMFS (DFS) spectra recorded setting BetP in a down-regulated state in absence (red) and in presence (green) of betaine, and in an up-regulated state in absence (black) and in presence of (blue) substrate. Buffer conditions were (blue) 400 mM KCl, 100 mM NaCl, 5 mM betaine, 50 mM Tris-HCl, pH 7.5, (black) 400 mM KCl, 100 mM NaCl, 50 mM Tris-HCl, pH 7.5, (green) 500 mM NaCl, 5 mM betaine, 50 mM Tris-HCl, pH 7.5, and (red) 500 mM NaCl, 50 mM Tris-HCl, pH 7.5. Shown are DFS spectra for all reproducibly occurring force peaks (interactions) as indicated in Fig. S1 and S2. Most probable forces and S.E. (error bars) of the DFS spectra were determined from the F-D curves superimposed in Fig. S5 and fits shown in Figs. S6–S9.

Table S1. Parameters characterizing the energy barriers (x_u, k_0, and ΔG_u) and spring constants (κ) of stable structural regions of BetP

	x_u (nm)				k_0 (s^{-1})			
Peak position / structural region	400 mM KCl 100 mM NaCl 5 mM betaine	400 mM KCl 100 mM NaCl no betaine (%)	500 mM NaCl 5 mM betaine (%)	500 mM NaCl (%)	400 mM KCl 100 mM NaCl 5 mM betaine	400 mM KCl 100 mM NaCl no betaine (%)	500 mM NaCl 5 mM betaine (%)	500 mM NaCl (%)
41 aa / N-terminal	0.35 ± 0.08	97	156***	135**	0.03 ± 0.06	43	16	21
58 aa / N-terminal	0.21 ± 0.04	141***	160**	146**	0.46 ± 0.50	11*	17	37
75 aa / TMH1	0.20 ± 0.03	106	199***	146***	0.56 ± 0.42	82	11**	65
92 aa / TMH2	0.14 ± 0.02	185**	157***	155***	3.04 ± 1.29	5***	45**	74
137 aa / Loop2★	0.23 ± 0.02	110**	111**	115**	0.18 ± 0.11	41**	146	99
154 aa / TMH3	0.19 ± 0.03	127*	123**	139***	0.97 ± 0.75	15**	81	61
184 aa / TMH4★	0.27 ± 0.05	75**	101	117*	0.17 ± 0.22	447***	422	113
242 aa / TMH5★	0.23 ± 0.03	101	119**	133***	0.22 ± 0.15	103	140	52
268 aa / Loop5	0.20 ± 0.01	110**	131***	174***	1.30 ± 0.43	61**	100	18***
285 aa / TMH6	0.45 ± 0.02	77***	77***	82***	0.02 ± 0.01	781*	1,219**	1,060**
324 aa / H7★	0.23 ± 0.02	133***	158***	151***	0.32 ± 0.16	18***	31***	37**
353 aa / Loop7	0.22 ± 0.03	154***	130**	142***	0.85 ± 0.61	4***	26**	13**
374 aa / TMH8	0.32 ± 0.06	106	73***	95	0.10 ± 0.12	43	1,291***	295
435 aa / EH2★	0.32 ± 0.02	100	211***	176***	0.13 ± 0.04	92	1***	6***
527 aa / TMH12★	0.63 ± 0.10	94	103	91	$(1.1 \pm 1.9) \times 10^{-3}$	183	303	808***
	ΔG ($k_B T$)				κ (N/m)			
Peak position / structural region	400 mM KCl 100 mM NaCl 5 mM betaine	400 mM KCl 100 mM NaCl no betaine (%)	500 mM NaCl 5 mM betaine (%)	500 mM NaCl (%)	400 mM KCl 100 mM NaC l5 mM betaine	400 mM KCl 100 mM NaCl no betaine (%)	500 mM NaCl 5 mM betaine (%)	500 mM NaCl (%)
41 aa / N-terminal	24 ± 1.9	104	108	107	1.60 ± 0.86	109	44**	59
58 aa / N-terminal	22 ± 1.1	110***	108	105	4.17 ± 1.92	56*	42**	49*
75 aa / TMH1	21 ± 0.7	101	111***	102	4.52 ± 1.51	90	28***	48***
92 aa / TMH2	20 ± 0.4	115**	104*	101	8.03 ± 2.33	34***	42***	42***
137 aa / Loop2★	22 ± 0.6	104**	98	100	3.60 ± 0.70	85	80**	76**
154 aa / TMH3	21 ± 0.8	109**	101	102	4.61 ± 1.62	68***	66*	53**
184 aa / TMH4★	23v1.3	93**	94*	99	2.50 ± 1.10	166	93	72
242 aa / TMH5★	22 ± 0.7	100	99	103*	3.52 ± 0.90	98	70**	59***
268 aa / Loop5	20 ± 0.3	102**	100	108***	4.36 ± 0.73	84	59***	36***
285 aa / TMH6	25 ± 0.4	92***	90***	91***	1.02 ± 0.11	153**	150**	134*
324 aa / H7★	22 ± 0.5	108***	105***	105**	3.44 ± 0.68	61***	42***	46***
353 aa / Loop7	21 ± 0.7	115***	106**	110***	3.51 ± 1.15	48***	63**	54**
374 aa / TMH8	23 ± 1.3	104	89***	95	1.88 ± 0.76	92	166***	106
435 aa / EH2★	23 ± 0.3	100	121***	113***	1.87 ± 0.22	101	27***	36***
527 aa / TMH12★	28 ± 1.8	98	96	92**	0.57 ± 0.22	110	90	111

Average values are shown for the energy barriers that stabilize structural segments of up-regulated BetP in the presence of substrate (400 mM KCl, 100 mM NaCl, 5 mM betaine, 50 mM Tris-HCl, pH 7.5). Relative to this reference values we give the percentage of the values reached for up-regulated BetP in the absence of substrate (400 mM KCl, 100 mM NaCl, 50 mM Tris-HCl, pH 7.5), and for down-regulated BetP in the absence (500 mM NaCl, 50 mM Tris-HCl, pH 7.5), and presence (500 mM NaCl, 5 mM betaine, 50 mM Tris-HCl, pH 7.5) of substrate. Differences compared to BetP characterized in 400 mM KCl, 100 mM NaCl, 5 mM betaine, 50 mM Tris-HCl, at pH 7.5 were considered being significant (printed in bold) when p-values approached <0.05 (**) and <0.01 (***) from T-student tests (Table S2) and their changes did not overlap within their standard deviations given in Table 1. Black star denote major force peaks that became dominant in superimposed F-D curves. Barrier heights, ΔG_u, and spring constants, κ, were calculated as described under *Calculation of Transition Barrier Heights and Rigidity* in the main text. Values that showed a significant difference are highlighted in bold. Errors of x_u and k_0 represent S.D. Errors in ΔG_u were estimated by propagating the errors of k_0. Errors in κ were estimated by propagating the errors of ΔG_u and k_0.

Table S2. Significance tests of the parameters characterizing the energy barriers (x_u, k_0, and ΔG_u) and spring constants (κ) of stable structural regions of BetP shown in Table S1

	x_u (nm)				k_0 (s^{-1})			
Peak position / structural region	400 M NaCl 5 mM betaine	400 mM KCl 100 mM NaCl no betaine	500 mM NaCl 5 mM betaine	500 mM NaCl	400 mM KCl 100 mM NaCl 5 mM betaine	400 mM KCl 100 mM NaCl no betaine	500 mM NaCl 5 mM betaine	500 mM NaCl
41 aa / N-terminal	1	0.872847	0.00329716	0.0200222	1	0.552632	0.311047	0.336676
58 aa / N-terminal	1	0.00391558	0.0155549	0.0357694	1	0.0711115	0.106877	0.257572
75 aa / TMH1	1	0.446525	3.43756e-05	0.00170222	1	0.625326	0.0162169	0.382327
92 aa / TMH2	1	0.0186122	0.00114362	0.00169552	1	0.000395443	0.0356449	0.381007
137 aa / Loop2★	1	0.031082	0.0185714	0.0168463	1	0.0419614	0.137326	0.978398
154 aa / TMH3	1	0.0587725	0.0115944	0.00147452	1	0.0266633	0.586397	0.278611
184 aa / TMH4★	1	0.010577	0.965546	0.0579745	1	0.00103535	0.141643	0.812225
242 aa / TMH5★	1	0.880703	0.0315657	0.000104753	1	0.93943	0.45119	0.136312
268 aa / Loop5	1	0.0470949	0.00601876	1.14471e-05	1	0.0398214	0.997074	0.000223172
285 aa / TMH6	1	0.00131506	0.000257939	0.00541371	1	0.0806264	0.011365	0.0441368
324 aa / H7★	1	6.0364e-05	1.83946e-06	7.43703e-05	1	0.00245037	0.00822501	0.0215358
353 aa / Loop7	1	0.000155937	0.0171738	0.00173648	1	0.00816458	0.0370472	0.0148292
374 aa / TMH8	1	0.649048	0.00490199	0.702561	1	0.392479	3.16416e-05	0.340131
435 aa / EH2★	1	0.899677	6.5664e-09	0.000253598	1	0.672154	2.66385e-05	5.68332e-05
527 aa / TMH12★	1	0.460586	0.709747	0.246565	1	0.465698	0.218655	0.00871962
	ΔG ($k_B T$)				κ (N/m)			
Peak position / structural region	400 mM KCl 100 mM NaCl 5 mM betaine	400 mM KCl 100 mM NaCl no betaine	500 mM NaCl 5 mM betaine	500 mM NaCl	400 mM KCl 100 mM NaCl 5 mM betaine	400 mM KCl 100 mM NaCl no betaine	500 mM NaCl 5 mM betaine	500 mM NaCl
41 aa / N-terminal	1	0.569673	0.128365	0.14809	1	0.827231	0.036602	0.110445
58 aa / N-terminal	1	0.0033091	0.105268	0.28841	1	0.0507205	0.0260658	0.0508724
75 aa / TMH1	1	0.613757	0.00387011	0.380352	1	0.539406	0.000495018	0.00651126
92 aa / TMH2	1	0.0207214	0.0545875	0.40868	1	0.00311245	0.00175753	0.00192303
137 aa / Loop2★	1	0.0130337	0.180852	0.978394	1	0.131969	0.0400688	0.0351838
154 aa / TMH3	1	0.0172623	0.561772	0.227815	1	0.133088	0.0507517	0.0122016
184 aa / TMH4★	1	0.0193368	0.0660209	0.821897	1	0.00795724	0.777115	0.156353
242 aa / TMH5★	1	0.939566	0.437348	0.0714028	1	0.888186	0.0441575	0.00296091
268 aa / Loop5	1	0.0382754	0.99707	0.000603862	1	0.108036	0.00309386	1.08222e-05
285 aa / TMH6	1	0.00164721	2.76865e-05	0.000270471	1	0.0388362	0.0136054	0.0904623
324 aa / H7★	1	0.000137275	0.00217928	0.0236687	1	0.00131706	5.36383e-05	0.000195871
353 aa / Loop7	1	5.76043e-05	0.020488	0.0016462	1	0.00475394	0.0466903	0.0121828
374 aa / TMH8	1	0.424526	0.000666426	0.214952	1	0.773996	0.00707222	0.861399
435 aa / EH2★	1	0.670857	7.62681e-08	0.00290417	1	0.871118	7.08404e-08	1.56891e-05
527 aa / TMH12★	1	0.501255	0.231732	0.0242589	1	0.602909	0.61304	0.551752

Values shown are *p*-values revealed from T-student tests of parameters given in Table 1.